CrossMark

JM PAPERS

Inside rod induced horizontal capillary emptying

Xinping Zhou[1,†], **Gang Zhang**[1,2], **Chengwei Zhu**[1,2], **Dongwen Tan**[1] **and Chenyu Fu**[1]

[1]School of Mechanical Science and Engineering, Huazhong University of Science and Technology, Wuhan 430074, PR China

[2]Department of Mechanics, Huazhong University of Science and Technology, Wuhan 430074, PR China

The removal of a liquid blockage from a tube is of importance in many processes. If the Bond number (which measures the relative size of the gravitational force by comparison with the surface tension force on the blockage plug) is large enough, then the tube will become non-occluding automatically. If not, then other measures are required to remove the blockage and the insertion of a rod is one such measure. We investigate this situation in a horizontal capillary in a downward gravity field. Theoretical results are obtained and compared with experiments. We observe that a rod insertion can cause a change from liquid plug to non-occlusion in a horizontal capillary. For uniform inner and outer contact angles, compared with the case without an inside rod, the maximum of the critical emptying line decreases significantly, but the minimum decreases a little only for a large enough value of the ratio of inner radius to outer radius (χ). We find that changing the contact angles of the inserted tube can significantly affect the non-occluding of the tube. The minimum of critical emptying line can be lowered clearly, and the minimum for a large enough value of χ is much lower than that reached for a circular tube. The insertion of a hydrophobic (hydrophilic) rod with a large enough radius can make the liquid emptying easier in a horizontal hydrophilic (hydrophobic) capillary. This provides an effective method of triggering drainage of a fluid from a capillary in applications such as optofluidics and microfluidics.

Key words: capillary flows

1. Introduction

Liquid or gas plugs may exist in small multiphase fluid containers, ranging from equipment in microgravity (Chen & Collicott 2006), devices in a gravity field (Zhang, Yang & Wang 2006) to cardiovascular vessels (Lee, Wu & Li 2020). Capillary plugs may degrade

---

† Email address for correspondence: xpzhou08@hust.edu.cn

the performance and, accordingly, it is essential to prevent fluid blockage in containers by capillary emptying (which is capillary non-occluding and does not mean the tube would completely empty here). A great deal of work has been done on determining the equilibrium shapes of liquid volumes in a tube of gas in microgravity, and the geometric parameters and wetting conditions have been studied to enhance the multiphase fluid performance (Concus & Finn 1969; Finn 1986; Smedley 1990; Chen & Collicott 2006; Pour & Thiessen 2019). In many situations, gravity has a significant effect on multiphase fluid interface deformation, which precedes the emptying of the capillary. The phenomenology of a capillary in a transverse gravity field is distinctively richer than that in micro gravity.

The primary parameter determining the presence or absence of a plug in a capillary is the Bond number $Bo = (\delta/l_{ca})^2$ where δ is the characteristic length of the capillary tube and $l_{ca} = \sqrt{\sigma/\rho g}$ is the capillary length, with the surface tension σ between liquid and gas, the density difference ρ between liquid and gas and the gravitational acceleration g. If the Bond number exceeds a critical value Bo_c then a plug will not arise. Other factors that affect the critical Bond number are the solid/liquid contact angle and the capillary geometry. Critical characteristic lengths of capillaries corresponding to the critical Bond numbers mainly range from millimetre sizes to micron sizes (see Parry *et al.* 2012), and are reduced to lower values at lower critical Bond numbers. Based on theoretical research, different cylinder cross-sections and contact angles have been proposed to help in preventing the existence of liquid plugs in a horizontal capillary in a downward gravity. A flattened ice-cream cone cylinder was designed by Manning, Collicott & Finn (2011), in which liquid non-occlusion will occur. Manning & Collicott (2015) concluded that, for a rectangular tube, a large enough width-to-height ratio of the cross-section can lead to the reduction of Bo_c. Other shapes (ellipse and triangle) and different orientations were found to be able to change Bo_c (Rascón, Parry & Aarts 2016).

In the recent work of our group (Zhu, Zhou & Zhang 2020), a strategy of setting the four linked wall surfaces of a horizontal rectangular capillary to have differing contact angles was proposed to reduce Bo_c as much as possible. It was found that Bo_c of a horizontal rectangular tube can be effectively decreased by decreasing the bottom and one side contact angles and increasing the top and the other side contact angles. Recently, Verma *et al.* (2020) performed several case experiments studying the emptying criteria for a finite-length rectangular tube (filled with water and a gas) with an open end and a closed end in a gravity field by considering the effect of the contact line pinning at the sharp edge, and it was shown that a different bottom contact angle from the top contact angle can lead to the change of Bo_c. This can validate the conclusions of Zhu *et al.* (2020) to some extent.

The three-dimensional (3-D) problem of (gas–liquid) two-phase fluids in a horizontal capillary in a downward gravity is complex to compute and study. Generally, researchers always tried to develop an analytic solution to the complex problem. Some special cases can be considered to be two-dimensional (2-D) and are easier to compute. Gas–liquid two-phase fluids confined in a horizontal wide capillary slit made of two parallel walls of length $L \gg H$ and width $W \gg H$ where H is the distance between the two walls, have essentially a 2-D gas–liquid interface. The distance between the two walls H and the height of rectangular cross-section are used as the characteristic lengths to calculate the Bond numbers in the plane case and in the rectangular case, respectively. A theoretical expression of the critical Bond number in the plane case was determined by Parry *et al.* (2012) as

$$Bo_c = 4\left(\sin\frac{\gamma_b}{2} + \cos\frac{\gamma_t}{2}\right)^2, \tag{1.1}$$

where γ_b and γ_t are the contact angles of the bottom and top walls, respectively. When the bottom and top walls have a uniform contact angle, that is, $\gamma_b = \gamma_t = \gamma$, the theoretical expression of Bo_c in the plane case can be reduced to

$$Bo_c = 4(1 + \sin\gamma). \tag{1.2}$$

Parry *et al.* (2012) experimentally studied the interfacial profiles of three samples in confinement between two parallel walls ($L = 15$ mm and $W = 0.5$ mm) with the distance between them $H = 0.062 \pm 0.001$ mm to demonstrate that an increase of Bond number allows for crossing the emptying phase boundary. Using numerical optimization scheme of Zhu *et al.* (2020) found that this analytic result works for rectangular capillary of a large width-to-height ratio providing the gas–liquid interface for the liquid non-occlusion state meets the two vertical walls so that the problem remains two-dimensional. If, however, the interface(s) for the non-occlusion state has two (four) contact points in one (two separated) corner region(s) then a modification is required; for more details see Zhu *et al.* (2020).

All the above findings for infinitely long 3-D capillaries (Manning *et al.* 2011; Manning & Collicott 2015; Rascón *et al.* 2016; Zhu *et al.* 2020) are based on theoretical research and little experimental work has been carried out. Evidently, a change in the cross-sectional shape will affect the emptying of a tube and the simplest possible shape change will result if a rod is inserted into the circular tube, effectively creating an annular tube. This is the situation we will investigate. Annular tubes are used in other fluid systems (for example, Smedley 1990; Pour & Thiessen 2019; Kang & Mutabazi 2021; Stokes 2021). It is noted that the use of eccentricity can avoid occlusion even at zero Bond number for ranges of radius ratio and eccentricity (Smedley 1990; Pour & Thiessen 2019). Although annular tubes are not more common than non-annular tubes, they can have higher performance in some applications under certain conditions. An annular structure created by inserting a rod into a tube maybe be a better choice in terms of capillary emptying. What happens when a rod is inserted into a horizontal capillary where a long liquid droplet plugs? At first thought, the plugging liquid droplet will become longer due to the pushing by the inserted rod, but that may not be the case because the equilibrium shape of liquid is reached at energy minimization. This is an interesting question but it has not been answered to date.

In this paper we investigate the effect of insertion of a rod on critical emptying conditions in a horizontal circular capillary and examine the effects of the inner-to-outer radius ratio and the uniformity and non-uniformity of the outer and inner contact angles on the critical emptying line. We organize this paper as follows. Section 2 describes the problem formation and the equations governing the equilibrium of the gas–liquid interface in a horizontal capillary. Experimental validation of the mathematical model is conducted in § 3. Results and discussion by considering the effect of the inner-to-outer radius ratio and contact angles are given in § 4. Finally, the conclusions are presented in § 5.

2. Problem formation and mathematical methods

Consider a horizontal rod inside a horizontal circular capillary of outer tube radius R_o and rod radius R_i partially filled with a liquid and a gas in a downward gravity field (see figure 1). The concentric annular tube is infinitely long and has a constant cross-section with its radius ratio being defined as $\chi = R_i/R_o$. The centroid of the concentric annulus lies on the x axis. The outer tube radius R_o is used as the characteristic length to define the Bond number of the system.

The macroscopic free energy of a liquid drop in a capillary includes the free surface energy, the wetting energy, the gravitational energy and a liquid internal energy term that
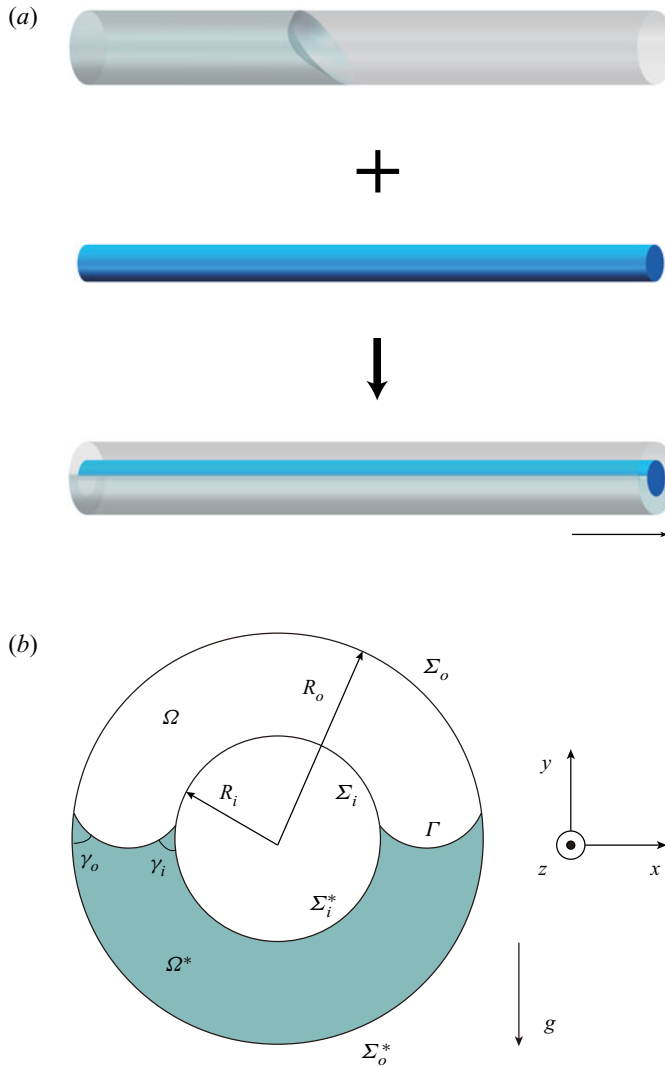
(*a*)

(*b*)

Figure 1. (*a*) Schematic of rod insertion into a horizontal circular capillary leading to change of a long liquid droplet from a plug to non-occlusion in a downward gravity field; (*b*) a cross-section of the horizontal concentric annular tube of inner and outer radii R_i and R_o with gas–liquid interface Γ, total and liquid interiors Ω and Ω^*, total and wetting inner perimeters Σ_i and Σ_i^*, total and wetting outer perimeters Σ_o and Σ_o^* and inner and outer contact angles γ_i and γ_o.

imposes a volumetric constraint on the problem. Under equilibrium conditions, the shape of the droplet is such that the total free energy is minimized.

In an infinitely long capillary, there are only two equilibrium states, that is, liquid plug and liquid non-occlusion. The effect of contact angle on the critical Bond number is normally presented in the form of a plot of critical Bond number as a function of contact angle and this plot is referred to as 'the critical emptying line'. The liquid tongue for the state of the liquid plug is finitely long and that for the state of liquid non-occlusion is infinitely long. The tongue gets longer with larger Bond number and becomes very long when the Bond number approaches the critical Bond number, as demonstrated by
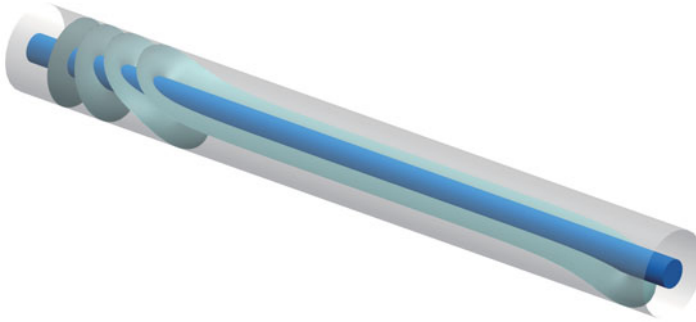
Figure 2. Schematic of evolution of the 3-D interface (an oblique view) as the Bond number gradually increases and approaches the critical Bond number. The 3-D interfaces computed by Surface Evolver (Brakke 1992) are integrated in a horizontal concentric annular tube.

the 3-D interfaces (see figure 2) directly computed via Surface Evolver (Brakke 1992); when the critical Bond number is attained, the tongue can be seen to be infinitely long and the cross-section intersected with the tongue can be seen to be translationally invariant. The total free energy of a 3-D droplet is finite. The total free energy per unit length of the tongue corresponding to the critical emptying line should be equal to 0. In this case, the 3-D problem can be reduced to an associated 2-D problem. The total free energy per unit length of liquid tongue based on a cross-section of an annular capillary is

$$\Phi = \Gamma - (\Sigma_o^* \cos \gamma_o + \Sigma_i^* \cos \gamma_i) + l_{ca}^{-2} \int_{\Omega^*} y \, \mathrm{d}x \, \mathrm{d}y + \lambda \Omega^*, \qquad (2.1)$$

where λ is a Lagrange parameter, Γ is the length of the gas–liquid interface (meniscus), Σ_o^* and Σ_i^* are the perimeters of the tube outer and inner walls in contact with the liquid, respectively, Ω^* is the liquid area and γ_i and γ_o are the inner and outer contact angles, respectively (see figure 1b). The critical emptying line can be determined when the below condition is satisfied (Finn 1986; Manning *et al.* 2011; Rascón *et al.* 2016):

$$\Phi = 0. \qquad (2.2)$$

The Young–Laplace equation describing the shape of a gas–liquid interface can be determined by minimization of the total free energy of the 3-D droplet. The Young–Laplace equation in two dimensions is given by (Bhatnagar & Finn 2016; Zhou & Zhang 2017)

$$\left(\frac{y_x}{(1 + y_x^2)^{0.5}} \right)_x = l_{ca}^{-2} y + \lambda. \qquad (2.3)$$

The Lagrange parameter λ can be obtained from integration of (2.3) as

$$\lambda = \frac{\Sigma_o \cos \gamma_o + \Sigma_i \cos \gamma_i}{\Omega} = \frac{2(\cos \gamma_o + \chi \cos \gamma_i)}{R_o(1 - \chi^2)}, \qquad (2.4)$$

where Ω is the cross-sectional area of the capillary. The numerical procedure is used as below. First, guess a value of the Bond number. The location of the three-phase contact point at the outer tube wall changes gradually from the lowest point to the highest point to calculate the gas–liquid interfaces by (2.3) with the contact angle conditions being satisfied and then obtain the value of the functional Φ from (2.1). Next, modify the value of the

Bond number based on the difference between the minimum value of the functional Φ and zero and then recalculate. The iteration computation is repeated until (2.2) is satisfied.

When the contact angles of the inner and outer walls of a horizontal concentric annular tube are uniform ($\gamma_o = \gamma_i = \gamma$), the Lagrange parameter λ can be reduced to

$$\lambda = \frac{2\cos\gamma}{R_o(1-\chi)}. \tag{2.5}$$

From the above equation, it is indicated that the concentric annular tube of outer radius R_o and radius ratio χ has a larger value of λ than the circular tube of radius R_o when the two tubes have the same contact angles.

For the uniform contact angle $\gamma_o = \gamma_i = 90°$, the constant λ is equal to 0, and the interface is a straight line on the x axis. By substituting the relevant parameters into (2.2), we obtain the theoretical critical Bond number as

$$Bo_c = \frac{3}{(\chi + 0.5)^2 + 0.75}. \tag{2.6}$$

The analytical expression for the critical Bond number given by (2.6) applies only for the case of inner and outer contact angles both equal to 90°. In the special case, the critical Bond number Bo_c is found to be equal to 3 for a horizontal circular capillary without an inside central rod, decreases with χ increasing and approaches the limit of 1 when $\chi \to 1$. This indicates that rod insertion can cause liquid emptying of a horizontal capillary (see figure 1*a*).

3. Experimental validation

Experiments were carried out to observe whether a long water droplet is in a plug or non-occlusion state before and after a rod is inserted into a long horizontal circular capillary tube. Both the tube of 20 cm in length and the rod of 30 cm in length were made of silica glass. The silica glass had a contact angle of approximately 30°. The two ends of the tube were open and, for the concentric annular tube case, the inside rod was hung on two accessories that were manufactured by 3D printing. The fluids in capillaries were exposed to two LED light sources. A Nikon D7200 camera mounted with Nikon Micro-NIKKOR 105 mm f/2.8G macro lenses was used to visualize the fluids in capillaries.

In the experiments for circular capillaries and concentric annular capillaries of inner-to-outer radius ratio $\chi \approx 0.5$, we used capillaries of different radii to vary the Bond number. We experimentally observe that the circular capillary is plugged by a long liquid droplet before a rod is inserted and, amazingly, the insertion of the rod leads to the emptying of the circular capillary when the Bond number is between Bo_c for circular capillary and Bo_c for concentric annular tube ($\chi = 0.5$) (see figure 3). This observation from the experiments of several samples basically coincides with the prediction of calculations using the mathematical model as presented in § 2 (see figures 3*b* and 3*c*). The capillaries are so long that the effect of the contact angle pinning at the sharp edge is negligible here.

4. Results and discussion

The critical Bond numbers of the concentric annular tubes of various inner-to-outer radius ratios χ ranging from 0 to 0.9 at an interval of 0.1 for the uniform contact angles ($\gamma_o = \gamma_i$) varying from 1° to 179° with an increment of 1° are shown in figure 4. The results for
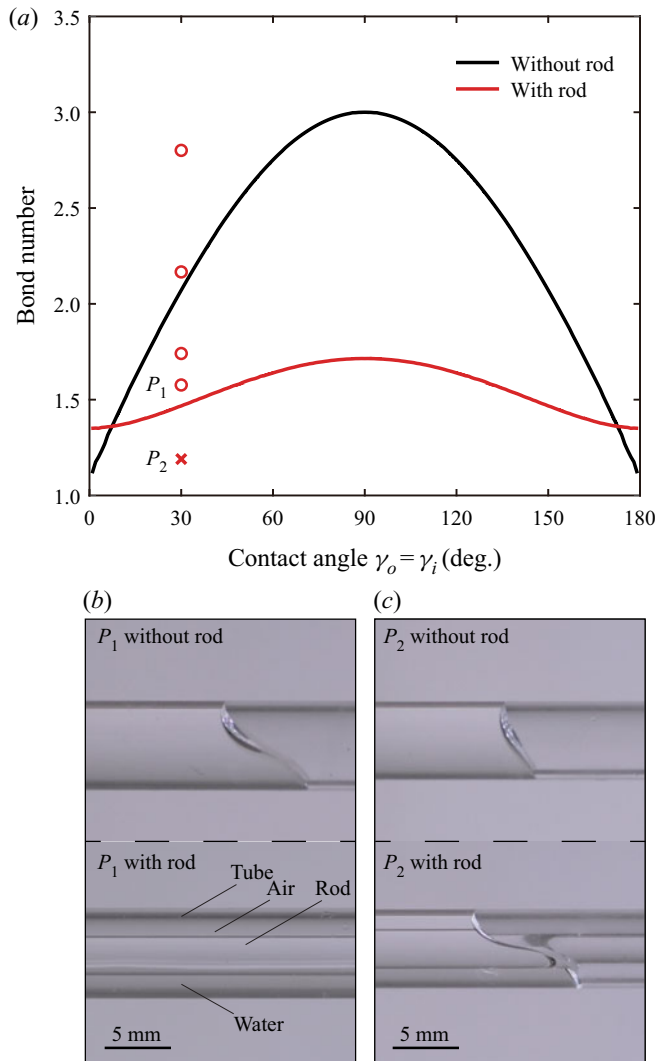
Figure 3. (*a*) Theoretical predictions for the 'critical emptying lines' ($Bo_c(\gamma)$ where $\gamma_o = \gamma_i = \gamma$) for the open capillary (upper black line), and for the capillary $\chi = 0.5$ with rod inserted (lower red line). Also shown are experimental results for a 6.79 mm diameter tube with rod inserted (P_1) and for a 5.92 mm diameter tube with rod inserted (P_2). Results are also presented for larger diameter capillaries again with inserted rods. The red circles indicate liquid non-occlusion and the red cross indicates that the liquid plug remains. Note that, as predicted by theory, the larger tube becomes non-occluding after rod insertion (see P_1) whereas the smaller tube remains blocked (see P_2). Panels (*b*) and (*c*) show photographs of the liquid plug or non-occlusion before and after rod insertion in the two cases P_1 and P_2.

$\chi = 0$ (representing a circular cylinder) are in excellent agreement with those calculated theoretically and directly computed via Surface Evolver (Brakke 1992) in 3-D mode, by Manning *et al.* (2011) and Rascón *et al.* (2016), independently. The calculated results for different values of χ for the cases $\gamma_o = \gamma_i = 90°$ are also in good agreement with the analytical solutions by (2.6) and those directly computed via Surface Evolver in 3-D mode, which again validates the model considering the effect of the radius ratio. As shown in figure 4, the insertion of a circular tube causes the reduction of Bo_c for a wide range of
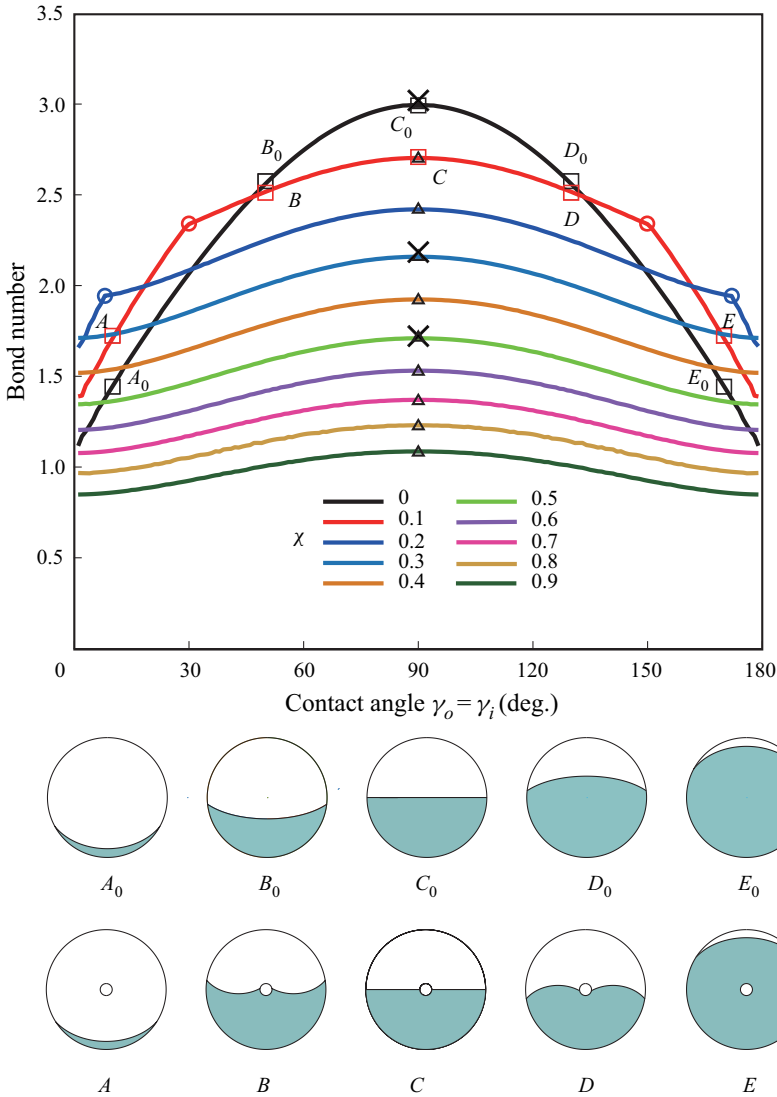
Figure 4. Critical Bond numbers of a horizontal circular tube ($\chi = 0$) and a horizontal concentric annular tube versus uniform contact angle $\gamma_o = \gamma_i$. The radius ratio of the concentric annular cylinder changes from 0.1 to 0.9. The triangles and the crosses denote the data calculated by (2.6) and those directly computed via Surface Evolver in 3-D mode, respectively, for $\gamma_o = \gamma_i = 90°$. The circles denote the kinks of the curves. The squares denote the representative points each corresponding to a cross-section of the part of the interface that extends to infinite length at the critical Bond number. Here, A_0, B_0, C_0, D_0 and E_0 correspond to $\gamma_o = \gamma_i = 10°$, $50°$, $90°$, $130°$ and $170°$, respectively, for the circular cylinder, while, A, B, C, D and E correspond to $\gamma_o = \gamma_i = 10°$, $50°$, $90°$, $130°$ and $170°$, respectively, for the concentric annular cylinder with $\chi = 0.1$.

contact angles for $\chi \leq 0.6$ (for example, from $47°$ to $133°$ for $\chi = 0.1$) and for all the contact angles for $\chi \geq 0.7$. Especially, it causes a large reduction of the maximum of Bo_c reached at $\gamma_o = \gamma_i = 90°$ and the reduction is more for larger radius ratio.

Figure 4 also gives the pictures, each of which represents a cross-section of the part of the interface extending to infinite length at the critical Bond number, for the circular cylinder and the concentric annular cylinder with $\chi = 0.1$, in the representative cases of
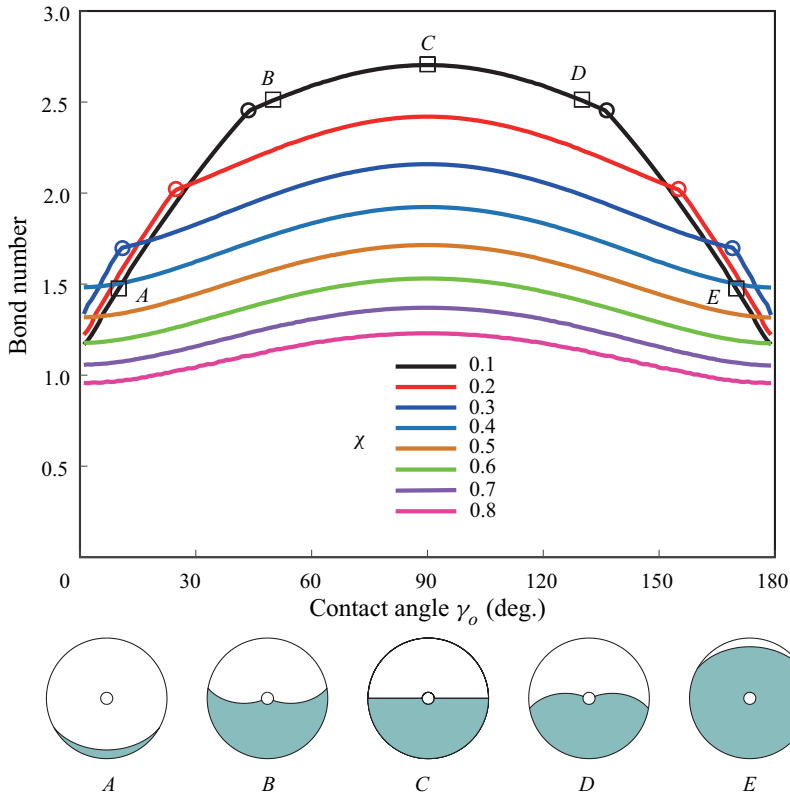
Figure 5. Critical Bond number of a horizontal concentric annular tube for inner wall contact angle $\gamma_i = 90°$ versus outer wall contact angle γ_o. The radius ratio of the concentric annular cylinder changes from 0.1 to 0.8. The circles denote the kinks of the curves. The squares denote the representative points each corresponding to a cross-section of the part of the interface that extends to infinite length at the critical Bond number. Here, A, B, C, D and E correspond to $\gamma_o = 10°$, $50°$, $90°$, $130°$ and $170°$, respectively, for $\chi = 0.1$.

$\gamma_o = \gamma_i = 10°$, $50°$, $90°$, $130°$ and $170°$. There exist three different non-occluded liquid topologies in a capillary with an inside concentric rod. For the type 1 topology (for example, the cross-section A), the gas–liquid interface is below the rod. For the type 3 topology (for example, the cross-section E), the interface is above the rod. The respective interfaces of the two topologies only meet the outer wall. For the type 2 topology (for example, the cross-sections B–D), the interface meets both the inner and outer walls. The interfaces for the three topologies are symmetric with respect to the vertical line of symmetry of the cross-section. This is attributed to both the uniformity of the contact angles on different linked parts of the outer wall and the uniformity of the contact angles on different linked parts of the inner rod.

For $\chi = 0.1$ and 0.2, with the uniform contact angle increasing, the type 1, 2 and 3 topologies occur in sequence. The type 2 topology corresponds to most of the contact angels, while the type 1 topology exists for small contact angles and the type 3 topology exists for large contact angles. Each of the two transitions between the type 1 topology and the type 2 topology and between the type 2 topology and the type 3 topology is accompanied by the occurrence of a kink of the Bo_c curve. With the increase of χ from 0 to 0.2, the minimum of Bo_c attained at $\gamma_o = \gamma_i = 1°$ or $179°$ increases. For $\chi = 0.3$–0.9, there only exists the type 2 topology. In this case, the curves of Bo_c become smooth and
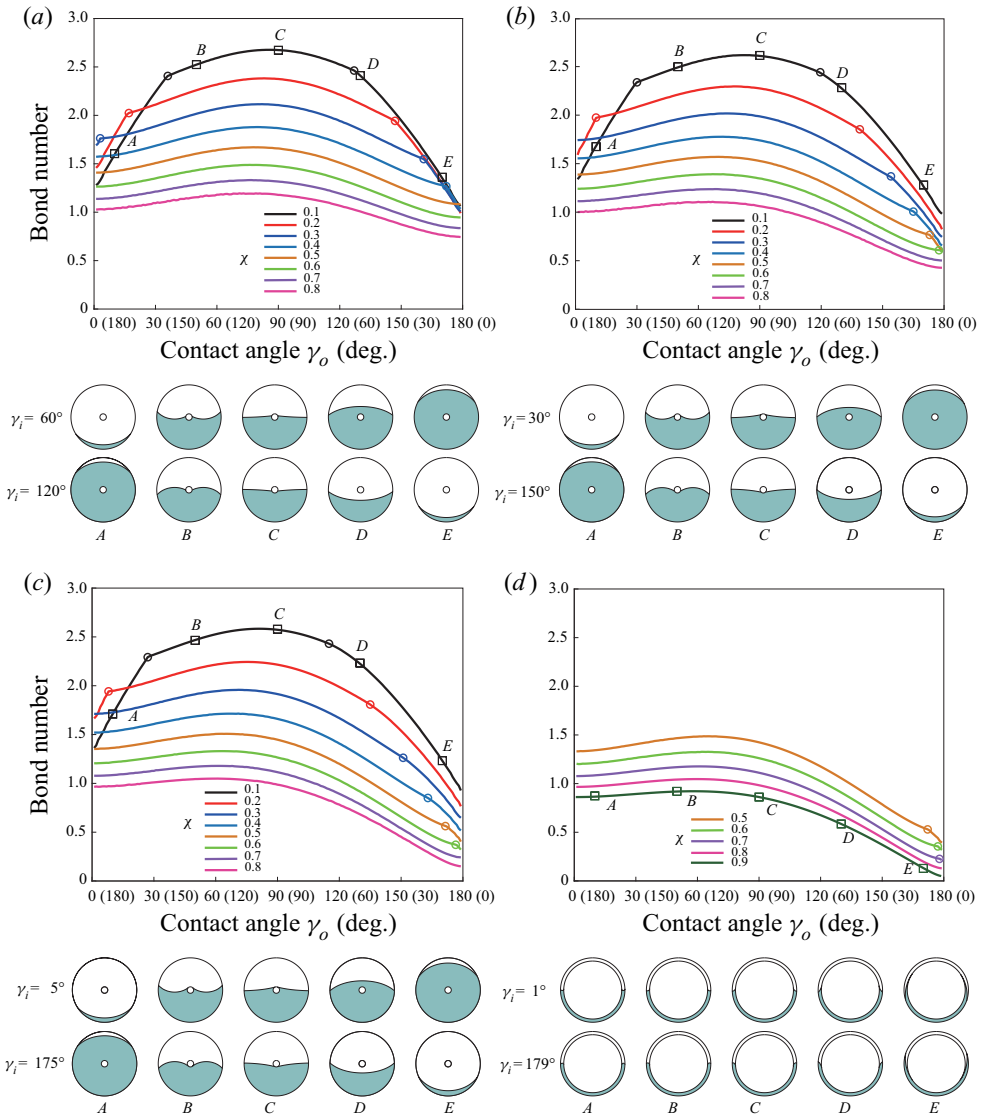
Figure 6. Critical Bond number of a horizontal concentric annular tube for inner wall contact angles $\gamma_i =$ (a) $60°$ $(120°)$, (b) $30°$ $(150°)$, (c) $5°$ $(175°)$ and (d) $1°$ $(179°)$ versus outer wall contact angle γ_o. The tick values outside the brackets on the horizontal axis correspond to the cases for $\gamma_i =$ (a) $60°$, (b) $30°$, (c) $5°$ or (d) $1°$, while those inside the brackets on the horizontal axis correspond to the cases for $\gamma_i =$ (a) $120°$, (b) $150°$, (c) $175°$ or (d) $179°$. In (a–c), different radius ratios from 0.1 to 0.8 are used and in (d) different radius ratios from 0.5 to 0.9 are used. The circles denote the kinks of the curves. The squares denote the representative points each corresponding to a cross-section of the part of the interface that extends to infinite length at the critical Bond number. Here, A, B, C, D and E on the upper (lower) row correspond to $\gamma_o = 10°$ $(170°)$, $50°$ $(130°)$, $90°$ $(90°)$, $130°$ $(50°)$ and $170°$ $(10°)$, respectively, for (a–c) $\chi = 0.1$ and (d) $\chi = 0.9$. In (a–d), the interfaces for A, B, C, D and E in the upper row are shown to be symmetrical to the interfaces for A, B, C, D and E in the lower row over the x axis, respectively.

the contact angle has a small influence on the value of Bo_c. With χ increasing from 0.3 to 0.9, the minimum of Bo_c gradually decreases, and the minimum for $\chi \geq 0.7$ becomes a little lower than the minimum for the circular tube. It is found that, for the cases of the

924 A23-10

uniform contact angles, the minimum critical Bond number is influenced to a small extent by changing the radius ratio of the tube.

Is it possible to further reduce the critical Bond number for a rod inside a capillary? We try to answer this question by setting different contact angles. In reality, it is easy to choose to use an inserted rod with a different contact angle from that of the capillary tube. We should examine the effect of changing the inside rod contact angle from the outer tube contact angle (which is different from the case of differing contact angles of four linked walls of the rectangle as shown in Zhu *et al.* 2020) on Bo_c. As shown in figure 4, Bo_c reaches the maximum at contact angles of $\gamma_o = \gamma_i = 90°$. By keeping γ_i constant ($= 90°$), the variations of Bo_c with the contact angle γ_o for different radius ratios are shown in figure 5. The curves are still symmetric about the vertical line $\gamma_o = 90°$. Compared with the circular tube, the maximum of Bo_c for the annular tube is reduced by an amount that increases with increasing radius ratio; however, the minimum reached at $\gamma_o = 1°$ or $179°$ is larger for $\chi \leq 0.6$ and a little smaller for $\chi \geq 0.7$. The three topologies exist for $\chi = 0.1$–0.3 but there is only the type 2 topology for $\chi \geq 0.4$. Compared with the case of equal inner and outer contact angles for a given radius ratio, the minimum of Bo_c is reduced by an amount that is very small for $\chi \geq 0.4$.

The interface for the case of γ_i and γ_o is found to be symmetrical to the interface for the case of $180°-\gamma_i$ and $180°-\gamma_o$ over the x-axis. Under these circumstances, based on (2.2), it is observed that the critical Bond number for the case of the inner wall contact angle γ_i and the outer wall contact angle γ_o is equal to that for the other case of the inner wall contact angle $180°-\gamma_i$ and the outer wall contact angle $180°-\gamma_o$. In order to further analyse the effect of the non-uniformity of γ_i and γ_o effectively, the inner wall contact angle is changed to $60°$ ($120°$), $30°$ ($150°$), $5°$ ($175°$) and $1°$ ($179°$), all of which are smaller (larger) than $90°$. The variations of Bo_c with the contact angle γ_o for different radius ratios and different inner wall contact angles are shown in figure 6. In this figure, the curves are not symmetric about the vertical line $\gamma_o = 90°$. As shown in figure 6(*a–c*), the minimum is attained at $\gamma_o = 179°$ ($1°$) and $\chi = 0.8$, and decreases with smaller (larger) value of γ_i. By further reducing (increasing) the inner wall contact angle to $\gamma_i = 1°$ ($179°$), the minima for $\chi \geq 0.8$ become lower than 0.13 and even the minimum for $\chi = 0.9$ is equal to approximately 0.058 (see figure 6*d*). In comparison with a circular tube and even a concentric annular tube of equal inner and outer contact angles, the minima are clearly reduced and the maxima are slightly reduced.

Unlike differing contact angles of four linked walls of a horizontal rectangular tube (Zhu *et al.* 2020), differing inner rod contact angles from the outer tube wall contact angle in the horizontal concentric annular tube never leads to the increase of the maximum critical Bond number but only decreases the minimum. It is concluded that the insertion of a hydrophobic circular rod with a large enough radius can make liquid emptying easier in a hydrophilic circular tube. The insertion of a hydrophilic circular rod with a large enough radius can also make liquid emptying easier in a hydrophobic circular tube.

5. Conclusions

In this paper, the effect of insertion of a rod on liquid emptying of a horizontal capillary in a downward gravity field is studied. The critical Bond numbers for the concentric annular tube for the cases with uniform inner and outer wall contact angles and the cases of differing inner rod contact angles from the outer tube contact angle are analysed, and the influence of the cross-section inner-to-outer radius ratio on the critical Bond number is examined.

Compared with the cases for a circular tube, for a concentric annular tube with uniform inner and outer contact angles, the maximum of Bo_c reached for the inner and outer wall contact angle $\gamma_i = \gamma_o = 90°$ decreases clearly, and the reduction is larger for larger radius ratio; however, the minimum is larger for a radius ratio smaller than or equal to 0.6 and a little smaller for a radius ratio larger than or equal to 0.7. An analytic formula with the radius ratio for calculation of the critical Bond number for $\gamma_i = \gamma_o = 90°$ is established. Differing inner rod contact angles from the outer tube contact angle causes the curves of Bo_c to be asymmetric about the vertical line $\gamma_o = 90°$ for $\gamma_i \neq 90°$. If $\gamma_i < (>) 90°$, the minimum is attained at $\gamma_o = 179°$ (1°) and decreases with the inner wall contact angle decreasing (increasing) and with the radius ratio increasing. The minimum attained at $\gamma_i = 1°$ and $\gamma_o = 179°$ (or $\gamma_i = 179°$ and $\gamma_o = 1°$) for a large enough radius ratio is much lower than that reached for a circular tube and a concentric annular tube of equal inner and outer contact angles. The insertion of a circular rod causes the occurrence of three topologies, including the type 2 topology with the interface meeting both the inner and outer walls and the other two topologies with the respective interfaces meeting the outer wall. A large enough radius ratio induces the type 2 topology to become the only occurring topology. The insertion of a large enough circular rod with the same wall surface property as the outer circular capillary may lead to the reduction of the minimum critical Bond number but the reduction is small. The insertion of a hydrophobic (hydrophilic) circular rod with a large enough radius can make the liquid emptying easier in a hydrophilic (hydrophobic) circular capillary. It is hoped that this paper would lay a solid foundation for design of non-occluding tubes in a transverse body force field.

Declaration of interests. The authors report no conflict of interest.

Author ORCIDs.
- Xinping Zhou https://orcid.org/0000-0001-6340-5273;
- Gang Zhang https://orcid.org/0000-0002-5236-4960.

References

BHATNAGAR, R. & FINN, R. 2016 On the capillarity equation in two dimensions. *J. Math. Fluid Mech.* **18**, 731–738.

BRAKKE, K.A. 1992 The surface evolver. *Exp. Maths* **1**, 141–165.

CHEN, Y. & COLLICOTT, S.H. 2006 Study of wetting in an asymmetrical vane-wall gap in propellant tanks. *AIAA J.* **44**, 859–867.

CONCUS, P. & FINN, R. 1969 On the behavior of a capillary surface in a wedge. *Proc. Natl Acad. Sci. USA* **63**, 292–299.

FINN, R. 1986 *Equilibrium Capillary Surfaces*. Springer-Verlag.

KANG, C. & MUTABAZI, I. 2021 Columnar vortices induced by dielectrophoretic force in a stationary cylindrical annulus filled with a dielectric liquid. *J. Fluid Mech.* **908**, A26.

LEE, C.C., WU, A. & LI, M. 2020 Venous air embolism during neurosurgery. In *Essentials of Neurosurgical Anesthesia & Critical Care: Strategies for Prevention, Early Detection, and Successful Management of Perioperative Complications*, pp. 287–291. Springer International Publishing.

MANNING, R.E. & COLLICOTT, S.H. 2015 Existence of static capillary plugs in horizontal rectangular cylinders. *Microfluid Nanofluid* **19**, 1159–1168.

MANNING, R., COLLICOTT, S. & FINN, R. 2011 Occlusion criteria in tubes under transverse body forces. *J. Fluid Mech.* **682**, 397–414.

PARRY, A.O., RASCÓN, C., JAMIE, E.A.G. & AARTS, D.G.A.L. 2012 Capillary emptying and shortrange wetting. *Phys. Rev. Lett.* **108** (24), 246101.

POUR, N.B. & THIESSEN, D.B. 2019 Equilibrium configurations of drops or bubbles in an eccentric annulus. *J. Fluid Mech.* **863**, 364–385.

RASCÓN, C., PARRY, A.O. & AARTS, D.G.A.L. 2016 Geometry-induced capillary emptying. *Proc. Natl Acad. Sci. USA* **113**, 12633–12636.

SMEDLEY, G. 1990 Containments for liquids at zero gravity. *Microgravity Sci. Technol.* **3**, 13–23.

STOKES, Y.M. 2021 A two-dimensional asymptotic model for capillary collapse. *J. Fluid Mech.* **909**, A5.

VERMA, G., SARAJ, C.S., YADAV, G., SINGH, S.C. & GUO, C. 2020 Generalized emptying criteria for finite-lengthed capillary. *Phys. Rev. Fluids* **5**, 112201(R).

ZHANG, F.Y., YANG, X.G. & WANG, C.Y. 2006 Liquid water removal from a polymer electrolyte fuel cell. *J. Electrochem. Soc.* **153**, A225–A232.

ZHOU, X. & ZHANG, F. 2017 Bifurcation of a partially immersed plate between two parallel plates. *J. Fluid Mech.* **817**, 122–137.

ZHU, C., ZHOU, X. & ZHANG, G. 2020 Capillary plugs in horizontal rectangular tubes with non-uniform contact angles. *J. Fluid Mech.* **901**, R1.